MOLECULAR AND CELLULAR BIOLOGY, Sept. 2005, p. 7828–7838 Vol. 25, No. 17
0270-7306/05/$08.00+0 doi:10.1128/MCB.25.17.7828–7838.2005

Abnormalities Caused by Carbohydrate Alterations in Iβ6-*N*-Acetylglucosaminyltransferase-Deficient Mice

Guo-Yun Chen,[1] Hisako Muramatsu,[1,2] Mineo Kondo,[3] Nobuyuki Kurosawa,[1] Yozo Miyake,[3] Naoki Takeda,[4] and Takashi Muramatsu[1,5]*

Department of Biochemistry,[1] Division of Disease Models, Center for Neurological Disease and Cancer,[2] and Department of Ophthalmology,[3] Nagoya University Graduate School of Medicine, Nagoya 466-8550, Center for Animal Resources and Development, Kumamoto University, Kumamoto 866-0811,[4] and Department of Health Science, Faculty of Psychological and Physical Sciences, Aichi Gakuin University, Aichi 470-0195,[5] Japan

Received 2 March 2005/Returned for modification 16 April 2005/Accepted 8 June 2005

Iβ6-*N*-acetylglucosaminyltransferase (IGnT) catalyzes the branching of poly-*N*-acetyllactosamine carbohydrate chains. In both humans and mice, three spliced forms of IGnT have been identified, and a common exon is present in all of them. We generated mice deficient in the common exon to understand the physiological function of poly-*N*-acetyllactosamine branching. IGnT activity was abolished in the stomach, kidney, bone marrow, and cerebellum of the deficient mice, while a low level of the activity persisted in the small intestine. Immunohistochemical analysis confirmed the loss of I antigen from the lung, stomach, and kidney. The deficient mice had reduced spontaneous locomotive activity. The number of peripheral blood lymphocytes was also reduced and renal function decreased in the deficient mice. Furthermore, in aged mice, vacuolization occurred in the kidney, and epidermoid cysts were frequently formed. However, cataracts did not develop earlier in the deficient mice. Decreased levels of lysosomal proteins, LAMP-2 and synaptotagmin VII, were found in the kidney of the deficient mice and correlated with renal abnormalities.

Protein-bound carbohydrates play essential roles in the regulation of cellular activities as epitopes recognized by other proteins and also as a factor defining the three-dimensional structure of the carrier protein (35). Poly-*N*-acetyllactosamines constitute a structural element of protein-bound carbohydrates and have repeated Galβ1-4GlcNAcβ1-3 units (8, 9, 35). They are present on the external portion of both *N*- and *O*-linked glycans. Poly-*N*-acetyllactosamine chains are often branched at C-6 of the galactosyl residue. The branched poly-*N*-acetyllactosamine chains become bulky and are good scaffolds for carbohydrate epitopes recognized by respective receptors (23, 33).

The branching of poly-*N*-acetyllactosamines is catalyzed by a specific β6-*N*-acetylglucosaminyltransferase (4, 20, 31), designated Iβ6-*N*-acetylglucosaminyltransferase (IGnT) based on the fact that the branched poly-*N*-acetyllactosamine structure is the basis of blood group I antigen (36). There are three isoforms of IGnT in both humans and mice designated IGnT A, B, and C or IGnT1, 2, and 3 (4, 6, 11, 20, 34, 40, 41). They are produced by alternative splicing of the IGnT gene (*Ignt*) (6, 11, 20, 34, 41); the unique portion is encoded by exon I, and the common portion is encoded by exons II and III (Fig. 1A).

The erythrocytes of most adults express I antigen. On rare occasions, erythrocytes have little I antigen and express i antigen (21), the epitope of which is a linear portion of poly-*N*-acetyllactosamines (36). The molecular basis of i blood group expression on erythrocytes has been clarified recently (11, 41); null mutations in IGnT C (IGnT3) are responsible for the phenotype. In Asians, the blood group i phenotype is associated with congenital cataracts (18, 28, 37), whereas the association is less pronounced in Caucasian populations (19, 22). Analysis of the IGnT gene has suggested that congenital cataracts are caused by null mutations of common exons (41). However, definitive proof and a mechanism that may cause cataracts in blood group i individuals remain to be provided.

Another interesting aspect of poly-*N*-acetyllactosamine branching is developmental change. Branched poly-*N*-acetyllactosamines are abundantly expressed in multipotential cells of early embryos and carry oncodevelopmental antigens such as Lewis X antigen (15, 23–25, 29). During embryogenesis, their expression progressively decreases (23). Fetal erythrocytes express i antigen but not I antigen due to a lack of poly-*N*-acetyllactosamine branching (8). Branched poly-*N*-acetyllactosamines in adult erythrocytes carry ABH blood group antigens (12, 16). These developmental changes imply some function of the branched structure during differentiation.

Given all of these considerations, we expected branched poly-*N*-acetyllactosamines to have significant roles in the generation and or function of various cells. In order to clarify the physiological significance and possible mode of action of branched poly-*N*-acetyllactosamines, we produced mice deficient in the common exon of the IGnT gene.

There is only one IGnT gene. However, core 2 β-6-*N*-acetylglucosaminyltransferase II (Core2GlcNAcT-II), the principal activity of which is to form core 2 branches in *O*-linked oligosaccharides, has a weak but significant level of activity to form branched poly-*N*-acetyllactosamines (38). Although Core2GlcNAcT-II has a restricted distribution and is not expressed in peripheral leukocytes and bone marrow in humans, it is strongly expressed in some human organs (38). Therefore, possible compensation by Core2GlcNAcT-II should be kept in mind when interpreting the phenotype of IGnT-deficient mice.

* Corresponding author. Mailing address: Department of Health Science, Faculty of Psychological and Physical Sciences, Aichi Gakuin University, Aichi 470-0195, Japan. Phone: 81-561-73-1111. Fax: 81-561-73-1142. E-mail: tmurama@dpc.aichi-gakuin.ac.jp.

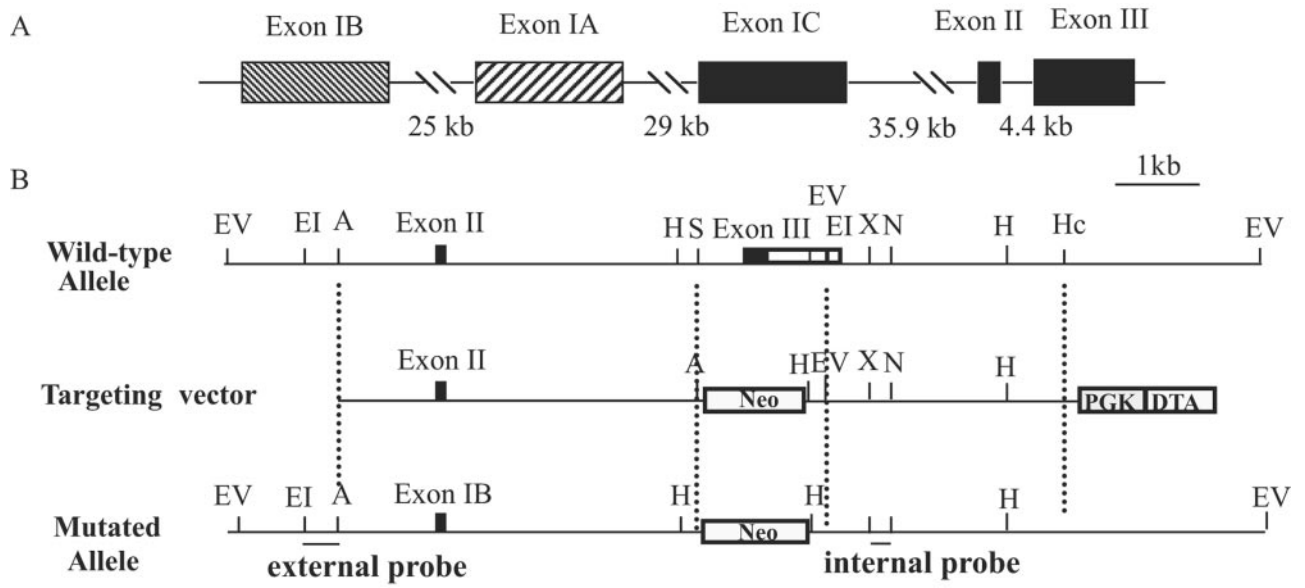

FIG. 1. Targeting strategy for the disruption of the IGnT gene. (A) Organization of the IGnT gene. Three forms of IGnT are present; they have one specific exon (exon I) and two common exons (exons II and III). Boxes show exons of the IGnT gene, and numbers show sizes of introns. (B) Construction of the targeting vector. A genomic DNA which contained exon II was used to construct the targeting vector. Positions of the external and internal probes used for Southern blot analysis are indicated. The restriction enzyme sites shown are as follows: EI, EcoRI; EV, EcoRV; A, ApaI; H, HindIII; S, SalI; X, XbaI; Hc, HincII; and N, NdeI. Closed boxes show the coding region, while open boxes show the noncoding region.

MATERIALS AND METHODS

Construction of the targeting vector. A genomic DNA clone, which encodes exon II and exon III of the IGnT gene and was isolated from a 129Sv/J genomic DNA library (6), was used to construct the targeting vector. The IGnT targeting vector was constructed from a basic targeting vector (10) with MC1neo (polyomavirus thymidine kinase gene promoter and neomycin resistance gene) and DTA (for diphtheria toxin fragment A gene) and fragments of IGnT genomic DNA (Fig. 1A). To delete a 2.0-kb portion of the DNA encoding exon III of IGnT (SalI-EcoRI sites in Fig. 1B), a 5.2-kb ApaI/SalI fragment, and a 3.6-kb EcoRI/HincII fragment in the genomic DNA clone were used as the 5′-arm and the 3′-arm, respectively (Fig. 1B).

Generation of targeted ES cells and mice. Aliquots of 20 μg of NotI-linearized targeting vector DNA were electroporated into 10^7 D3 embryonic stem (ES) cells. The cells were plated on mitomycin C-treated G418-resistant SL-10 cell feeder layers. G418 (250 μg/ml; Sigma) was added 24 h after plating. G418-resistant colonies were recovered after 7 to 8 days and then propagated to be stored and examined for homologous recombination by Southern blot analysis as described below. ES cells of the targeted clones were injected into blastocysts derived from naturally mated C57BL/6J females. The injected embryos were transferred to the uteri of pseudopregnant ICR mice. Chimeras were mated with C57BL/6J females, and homozygous deficient mice (F_1 generation) were generated by the intercrossing of heterozygotes. Genotypes were determined by tail DNA-PCR by using the IGnT gene exon III as a wild-type allele-specific probe, and the *neo* gene as a mutant allele-specific probe. IGnT-deficient mice were backcrossed to C57BL/6J mice four times, and heterozygotes were again crossed with each other to obtain the deficient and wild-type mice. Littermates of deficient (F_1 or F_5 to F_8) and wild-type mice were used for analysis.

Southern and Northern blot analyses. Southern blot analysis was performed as described previously (6). Genomic DNA from ES cells or the liver was isolated, digested with EcoRV or HindIII and after electrophoresis was transferred onto a nylon membrane. The membrane was hybridized with a 0.9-kb EcoRI/ApaI external probe or a 0.6-kb XbaI/NdeI internal probe (Fig. 1B). The homologously recombined DNA gave an 18.3-kb band or a 2.6-kb band, whereas the wild-type DNA gave a 9.2-kb band or a 4.8-kb band, respectively (Fig. 2A and B). Total RNA prepared from the liver was electrophoresed and transferred onto a nylon membrane and then hybridized with the radioactive probe as described previously (6). Hybridization was performed by using a 1.2-kp DNA fragment corresponding to full-length cDNA of the IGnT B gene as a probe.

PCR. Aliquots of 0.1 μg of DNA were mixed with 25 μl of 1× ExTaq buffer containing 0.2 mM concentrations of each deoxynucleoside triphosphate, 1.5 mM $MgCl_2$, 10 pmol of each primer, and 0.5 U of ExTaq DNA polymerase (Takara, Tokyo, Japan). PCR amplification was carried out at 96°C for 2 min, with 35 cycles of 96°C for 20 s, 59°C for 30 s, and 72°C for 150 s. To screen for homologously recombined DNA, the following IGnT primers were used: 5′-GATTGTAGGTCATTCCAGATAGAGTCA-3′ (IGnT KO-sense) and 5′-TCACAGGTTCCAGACCCACACAGTAGC-3′ (IGnT KO-antisense). The wild-type allele gave a 2.1-kb band, whereas the mutated allele gave a 1.3-kb band. The following Neo primers were also used: 5′-AGCTGTGCTCGACGTTGTCACTGA-3′ (Neo-sense) and 5′-CGCATTGCATCAGCCATGATG-3′ (Neo-antisense). The wild-type allele gave no band, whereas the mutated allele gave a 129-bp band.

Reverse transcriptase-mediated PCR (RT-PCR). Total RNA was isolated from the kidney, cerebellum and leukocytes of wild-type mice by the ISOGEN method (Wako-Chem, Osaka, Japan). Poly(A)$^+$ RNA was purified by using the Oligotex-dT30 (Takara). cDNAs were made from total poly(A)$^+$ RNA by using the Superscript first-strand system (Invitrogen). The PCR conditions were 94°C for 30 s, 58°C for 30 s, and 72°C for 30 s for 35 cycles. The primers for IGnT were CAGCCTATCTCTCATTGCTGC and TAAATGGCCCTGAAGAGTCTC. The primers for glyceraldehyde 3-phosphate dehydrogenase (G3P) were AAGGTCATCCATGACAAC and CACCCTGTTGCTGTAGCCA.

Isolation of B lymphocytes, T lymphocytes, and granulocytes for RNA preparation. B cells and T cells were isolated from suspended single cells from the spleen. For B cells, 2×10^8 spleen cells in 900 μl of the separation buffer (Dulbecco phosphate-buffered saline [PBS] containing 0.5% bovine serum albumin [BSA] and 2 mM EDTA) was mixed with 100 μl of anti-CD45R (B220) MicroBeads (Miltenyi Biotec, Auburn, CA), followed by incubation for 15 min at 4°C. For T cells, 2×10^8 spleen cells in 450 μl of the separation buffer was mixed with 50 μl of R phycoerythrin (PE)-conjugated anti-CD3 (BD Biosciences, Bedford, MA), followed by incubation for 30 min. After five washes with the buffer, cells were resuspended in 900 μl of the buffer. The cell suspension was mixed with 100 μl of anti-PE MicroBeads (Miltenyi Biotec) and incubated for 30 min at 4°C. The labeled B cells or T cells were then isolated by magnetic separation by using MACS LS column and MACS separator (Miltenyi Biotec) according to the manufacturer's instructions. Granulocytes were isolated from peripheral blood. A total of 4 ml of the blood was carefully layered onto 3 ml of Ficoll-Paque Plus (Amersham Biosciences) and centrifuged at 400 × *g* for 40 min. After the

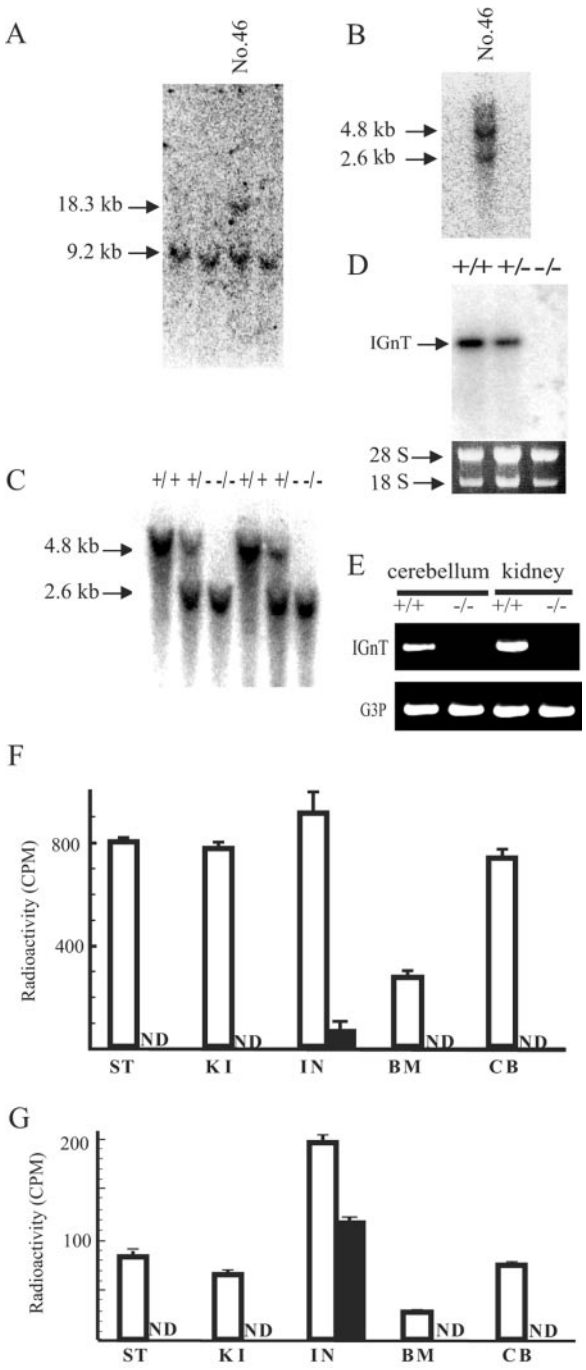

FIG. 2. Analyses to demonstrate deletion of the IGnT gene. (A, B and C) Southern blot analysis. (A) DNA from ES cells was digested with EcoRV and hybridized with the external probe. (B) DNA from ES cells was digested with HindIII and hybridized with the internal probe. (C) DNA from the liver of F_1 mice was digested with HindIII and hybridized with the internal probe. The expected DNA fragments for the mutant allele and the wild-type allele are indicated. (D) Northern blot analysis. Total RNA from the liver was analyzed by using an IGnT B probe. 28S and 18S rRNAs are shown as loading controls. (E) RT-PCR analysis to detect IGnT mRNA in the cerebellum and kidney. (F and G) Assay of IGnT enzymatic activities using lacto-*N*-neotetraose (F) and GlcNAcβ1-3Galβ1-4Glc (G) as substrates. The results are shown as radioactivity transferred to the product by enzyme extracts from the following organs: ST, stomach; KI, kidney; IN, intestine; BM, bone marrow; and CB, cerebellum. Bars: □, activity in wild-type mice; ■, activity in deficient mice. ND, not detected (<30 cpm). Eight-week-old, male F_1 mice were used for analysis of mRNA and enzymatic assay except that in panel E F_8 mice were used.

upper layer and the lymphocyte layer were removed, the pellet, which contained granulocytes and erythrocytes, was suspended in 10 ml of erythrocyte lysis buffer (QIAGEN, Hilden, Germany) for 10 min at room temperature and washed with PBS three times.

Assay of IGnT activity. Mouse tissues were removed and then homogenized with a Dounce homogenizer in 1.5 ml of 10 mM Tris-HCl buffer (pH 7.2), containing 0.25 M sucrose and 0.5% Triton X-100. The homogenates were centrifuged at 10,000 × *g* for 15 min, and the activity of IGnT in the supernatant was determined by using lacto-*N*-neotetraose as a substrate as described previously (6). The amount of protein added to the reaction mixture was 200 μg, and the enzymatic reaction was allowed to proceed for 15 h. For determination of predistal acting IGnT activity, the substrate was replaced with GlcNAcβ1-3Galβ1-4Glc, which was prepared from lacto-*N*-neotetraose by β-galactosidase digestion (6).

Behavioral analysis. Spontaneous activities were recorded automatically in a computerized activity-tracing chamber (Actimo-100, S/N 0000015; Eikou Science, Tokyo, Japan) for 24 h. The mice used were littermates of the F_5 generation and 12 weeks old. For the rota-rod test, a plastic rota-rod was used, driven by a small electric engine (Rota-Rod Treadmill for mice, MK-600; Muromachi Kikai Co. Ltd., Tokyo, Japan). Mice were placed onto the rod, and the rod was rotated at 10 rpm. The retention time on the rod was automatically recorded. The mice were given 3 days training before the experiment was performed.

Immunohistochemistry and staining. Tissues from wild-type or deficient mice were fixed in 4% paraformaldehyde, dehydrated, and embedded in paraffin according to the standard procedure. Sections of 5 μm were made and stained with hematoxylin-eosin (HE) or reacted with anti-I monoclonal antibody OSK14 (human immunoglobulin M [IgM]) or with anti-Lewis X monoclonal antibody 4C9 (rat IgM) (27, 39) for 1 h at room temperature. OSK14 antibody was produced and kindly provided by T. Yamano, Osaka Red Cross. The sections were washed in PBS and subsequently incubated with the second antibody, horseradish peroxidase (HRP)-conjugated goat anti-rat or human IgM (Sigma, St. Louis, MO), for 30 min at room temperature. After being washed in PBS, slides were developed with 3,3′-diaminobenzidine and counterstained with hematoxylin. In some experiments the second antibody was replaced with fluorescein isothiocyanate (FITC)-conjugated $F(ab')_2$ fragment of rabbit anti-human IgM (Dako, Glostrup, Denmark) specific for μ-chains. For the control, immunohistochemical staining was performed by omitting the primary antibody. No significant staining was observed upon control staining.

Flow cytometric analysis. After mincing of the spleen in PBS, single-cell suspensions were prepared in ice-cold PBS containing 1% BSA. Blood cells and single-cell preparation from the spleen were treated with Tris-ammonium chloride buffer (pH 7.2) and then incubated at 4°C for 15 min in 10 μg of Fc blocker (anti-CD32/16, 2.4G2; Pharmingen, San Diego, CA)/ml before being stained with antibodies. Cells were stained for 30 min at 4°C in the same buffer containing diluted antibody and then washed with the buffer. A FACSCalibur flow cytometer and CellQuest software (Becton Dickinson) were used to analyze the stained cells. FITC-labeled antibodies against CD3 and B220 (RA3-6B2) were from Pharmingen. For two color analysis, cells were stained by PE-labeled antibody against CD3, B220 (Pharmingen) or Gr-1 (Miltenyi Biotech) and OSK 14 antibody, followed by FITC-conjugated $F(ab')_2$ fragment of rabbit anti-human IgM specific for μ-chains.

Analysis of blood. Blood was obtained from age-matched male littermates through a tail vein. The 2-month-old mice were of the F_5 generation, and 6-month-old mice were of the F_1 generation. The total numbers of red blood cells and white blood cells were counted. Neutrophils, lymphocytes, and monocytes were counted manually after the staining blood smears with Wright-Giemsa. Blood urea nitrogen (BUN) was determined by the urease-glutamate dehydrogenase assay using a Fuji Dri-Chem slide system (Fujifilm, Tokyo, Japan). The serum creatinine concentration and serum glucose concentration were also determined by using the Fuji Dri-Chem slide system.

Western blot analysis. One kidney from wild-type or deficient mice was homogenized in 1.5 ml of 10 mM Tris-HCl buffer (pH 7.2) containing 0.25 M sucrose and 0.5% Triton X-100. After centrifugation, proteins in the extract were separated by sodium dodecyl sulfate-polyacrylamide gel electrophoresis (SDS-PAGE) and transferred onto a nitrocellulose membrane. The concentration of running gel was 10% unless specified otherwise. After blocking with 5% skim milk, the blots were incubated with rat anti-mouse LAMP-1 monoclonal antibody (Santa Cruz Biotechnology), rat anti-mouse LAMP-2 monoclonal antibody

(Santa Cruz Biotechnology), goat anti-mouse synaptotagmin II antibody S-15 (Santa Cruz Biotechnology) and goat anti-human synaptotagmin VII antibody N-18, which cross-reacts with the mouse antibody (Santa Cruz Biotechnology) or OSK-14 antibody. After incubation with the second antibody (HRP-conjugated goat anti-rat IgG, rabbit anti-goat IgG, or goat anti-human IgM), the signal was detected with an ECL kit (Amersham Biosciences). For the control, the membrane was deprobed and rehybridized with anti-β-actin (Pharmingen).

Immunoprecipitation. Extracts were prepared from the kidney of wild-type or deficient mice as described in the above section and were diluted fivefold with PBS that included protease inhibitors (1 μg of leupeptin/ml, 1 μg of aprotinin/ml, and 1 mM phenylmethylsulfonyl fluoride). An equal amount of the extract (1 mg of protein) was incubated with 20 μl of anti-LAMP-2 antibody (Santa Cruz Biotechnology) with gentle shaking for overnight at 4°C. Samples were then mixed with 60 μl of protein A-conjugated agarose beads (Upstate, Lake Placid, NY) for 2 h at 4°C, and immunoprecipitates were washed four times with PBS and resuspended in an SDS sample buffer for Western blot analysis.

Assay of antibody production. Three-month-old mice (two males and one female for a genotype) were immunized intraperitoneally with 100 μg of ovalbumin in PBS with Freund complete adjuvant. After 3 weeks, the second immunization was performed with 50 μg of ovalbumin in PBS with Freund incomplete adjuvant. The titer of the antibody was determined by an enzyme-linked immunoassay in which 100 ng of ovalbumin in PBS was coated per a well, 0.1% BSA in PBS was used as a blocking reagent, and HRP-conjugated sheep anti-mouse IgG (Jackson Immunoresearch Laboratories, West Grove, PA) was used as the second antibody.

Examination of cataracts. The mouse lens was examined without anesthesia in order to avoid the influence of anesthetic drugs on the lens' opacity. Biomicroscopic images were obtained by directing a narrow optical section of light along the polar axis of the lens. Slit-lamp images of the mouse lens were photographed with a slit-lamp microscope system (Kowa SC-1200; Kowa, Hamamatsu, Japan). Lens opacity was scored according to the system outlined in previous studies (7, 13): 0, clear normal lens; 1, peripheral vesicle and minimal cortical opacity; 2, peripheral vesicle and moderate cortical opacity; 3, diffuse central opacity; and 4, nuclear opacity, including cortical fiber change.

Statistical analysis. Data are presented as the means ± the standard errors of the mean. The number of determinations in a mouse was 3. Statistical significance was assessed by using Student *t* test.

RESULTS

Generation of IGnT-deficient (*Ignt*$^{-/-}$) mice. All three spliced forms of IGnT share common exons, exon II and III (Fig. 1A). We designed a targeting construct to delete part of the catalytic region encoded by exon III, together with the flanking sequence (Fig. 1). Using standard gene knockout technology, mice with a deletion of the IGnT gene (*Ignt*$^{-/-}$) were produced. By mating *Ignt*$^{+/-}$ mice, *Ignt*$^{-/-}$ mice were born with the Mendelian ratio. Southern blot analysis confirmed that the IGnT gene was deleted in the deficient mice (Fig. 2A, B, and C), and no IGnT mRNA was detected in the liver of IGnT-deficient mice, indicating that IGnT A, B, and C were deleted together (Fig. 2D). Disappearance of IGnT transcript in the cerebellum and kidney was also shown by RT-PCR (Fig. 2E). No significant differences were observed in the body weight of *Ignt*$^{-/-}$ mice as compared to *Ignt*$^{+/+}$ mice, 9, 10, 11, 12, 13, 15, or 19 weeks after birth (data not shown). When IGnT-deficient mice were mated with each other, they reproduced normally.

IGnT activity and I antigenic activity of IGnT-deficient mice. No IGnT or related activity was detected, when homogenates of the stomach, kidney, bone marrow, or cerebellum from IGnT-deficient mice were used as enzyme sources, although homogenates of these organs from the wild-type mice exhibited significant activity (Fig. 2F). However, a low level of the transferase activity was still detected in homogenate of the small intestine from the deficient mice. This activity was considered to be due to Core2GlcNAcT-II, which is strongly expressed in the human small intestine (38), or to other enzymes. To examine this point, we used another substrate, GlcNAcβ1–3Galβ1–4Glc, instead of the ordinary substrate, Galβ1-4GlcNAcβ1–3Galβ1–4Glc; in both cases, branches are formed at the underlined galactose residues. IGnT activities are classified to central acting one and predistal acting one (38). The activity determined by the latter substrate corresponds to that of central acting one (6), while the activity determined by the former substrate corresponds to that of the predistal acting one. Core2GlcNAcT-II has stronger predistal acting activity than central acting activity, whereas IGnT enzyme exhibits stronger central acting activity than the predistal acting one (38). Indeed, predistal acting activity measured using the trisaccharide substrate became more prominent in the small intestine, and the majority of the activity persisted in the small intestine of the deficient mice (Fig. 2G), confirming that the remaining activity in the small intestine of the deficient mice was due to Core2GlcNAcT-II.

We also performed immunohistochemical staining to detect I antigen using a monoclonal antibody OSK-14. In wild-type mice, I antigen was found in the alveoli of the lung, the luminal aspect of the tubules in the kidney and cells facing the luminal surface of the stomach (arrows in Fig. 3A, C, and E). The corresponding tissue in the IGnT-deficient mice lacked the antigenic expression (Fig. 3, B, D, and F). However, in the small intestine, I antigen was detected in the Paneth cells and serosa of the intestine at decreased levels in the deficient mice compared to wild-type mice (shown by arrows, Fig. 3G and H). The persistence of I antigen in the small intestine is consistent with the residual enzyme activity due to Core2GlcNAcT-II in the organ. Since Core2GlcNAcT-II is strongly expressed in the human stomach (38), we also performed indirect immunofluorescence staining of the stomach and confirmed that I antigen expression in the stomach (Fig. 3J) was abolished almost completely in the deficient mice (Fig. 3L). Absence of IGnT activity including the predistal acting one in the stomach of the deficient mice (Fig. 2F and G) was consistent with the immunohistochemical findings. We considered that Core2GlcNAcT-II was not expressed at significant levels in the stomachs of mice.

I antigen was not detected in the cerebellum in either wild-type or deficient mice (Fig. 3M and N). However, expression of 4C9 antigen, the epitope of which is Lewis X, was found in the glomeruli of the granular layer of the cerebellum, and the expression was significantly decreased in the deficient mice (Fig. 3O and P). Except for the cerebellum, 4C9 antigenic activity was not found in the brain (data not shown).

Reduced spontaneous activity in IGnT-deficient mice. When spontaneous activity was recorded automatically in a computerized activity-tracing chamber, the mutant mice showed significantly reduced activity in total, in the daytime, and in the nighttime compared to wild-type mice (Table 1). Both male and female mice were affected (Table 1). Although rota-rod tests were performed to examine motor coordination, no difference was observed between wild-type mice and the deficient mice in this respect (data not shown). The result suggested that the reduced spontaneous activity was not due to decreased motor coordination.

Decreased lymphocyte population in peripheral blood of IGnT-deficient mice. Although the number of erythrocytes did not differ, the number of white blood cells was decreased in

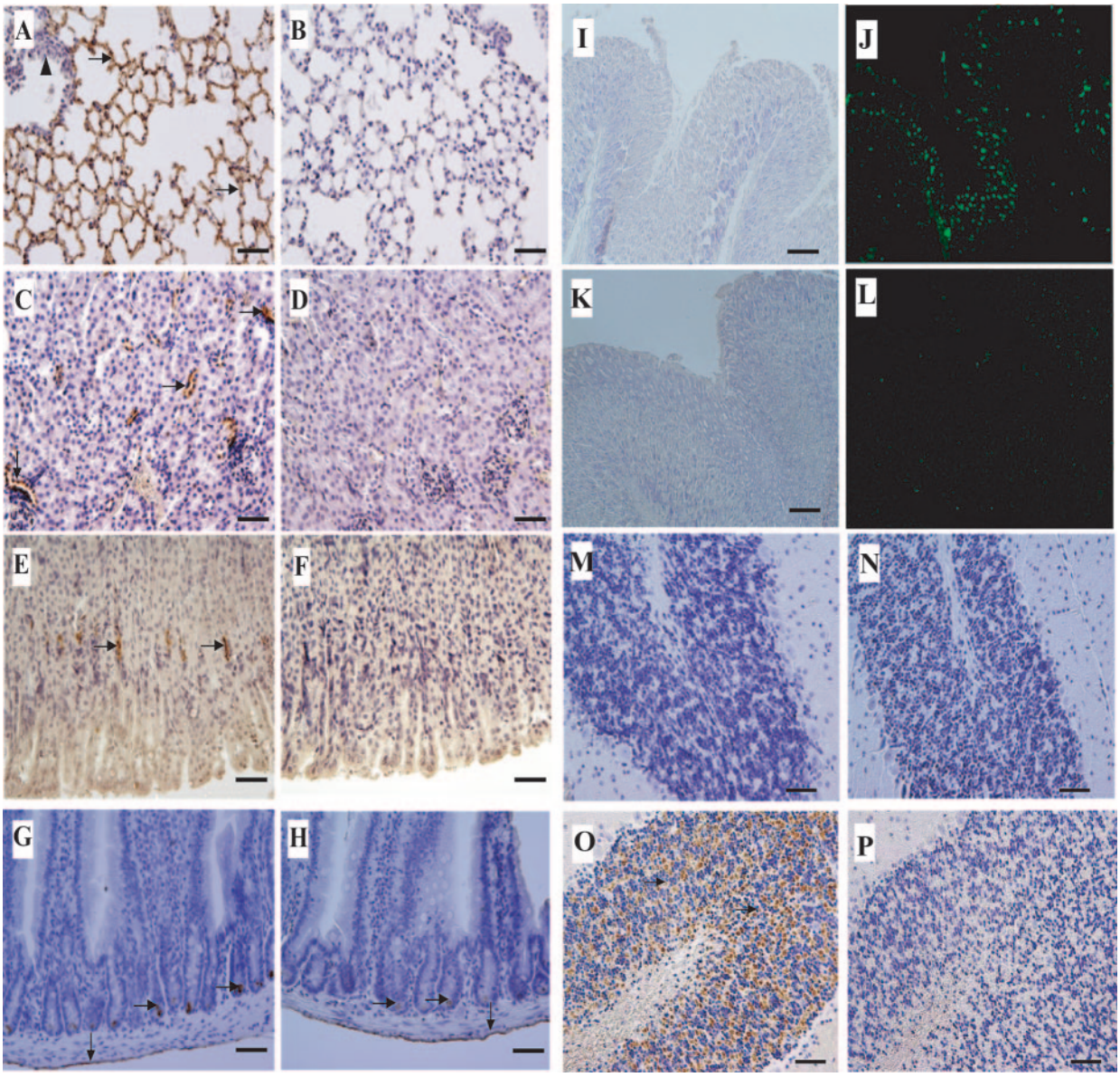

FIG. 3. Immunohistochemical analysis to detect I antigen and 4C9 Lewis X antigen. Slices from the lung (A and B), kidney (C and D), stomach (E and F), and small intestine (G and H) were stained with OSK-14 anti-I antibody and counterstained with hematoxylin. Serial sections from the stomach were also stained with hematoxylin (I and K) or OSK-14 anti-I antibody (J and L). Slices from the cerebellum were stained with OSK-14 anti-I antibody (M and N) or 4C9 anti-Lewis X antibody (O and P) and counterstained with hematoxylin. Arrows show positive signals. An arrowhead shows the bronchioles, which were not stained by anti-I antibody. The second antibody used was horseradish peroxidase labeled, except that in panels J and L, it was FITC labeled. Panels A, C, E G, I, J, M, and O show samples from wild-type mice; panels B, D, F, H, K, L, N, and P show samples from deficient mice. Tissues were taken from 8-week-old male mice, except the cerebellum images which were taken from 2-week-old male mice. Bar, 50 μm.

both the 2-month-old and the 6-month-old deficient mice (Table 1). This decrease was almost entirely accounted for by the decrease in lymphocytes (Table 1); the number of neutrophils and that of monocytes did not decrease. When the percentages of T cells and B cells among peripheral blood lymphocytes of 2-month-old F_5 mice ($n = 6$, each genotype) were compared, the values were 28.8 ± 11.5 and 52.8 ± 8.9, respectively, for wild-type mice. The values were 36.2 ± 4.3 and 41.8 ± 10.3, respectively, for the deficient mice. Considering the decrease of total number of lymphocytes in the deficient mice, we concluded that the number of B cells decreased in the deficient mice, and the number of T cells did not change significantly. Thus, the principal cause of the decrease in numbers of white blood cells was the decrease in the numbers of B cells.

We analyzed expression of I antigen in B cells, T cells, and granulocytes isolated from the spleen (Fig. 4). Most of the B cells expressed the antigen, and the significant fraction expressed the antigen strongly (Fig. 4B). A part of the T cells weakly expressed the antigen, and the rest were negative (Fig. 4D). The majority of granulocytes expressed the antigen (Fig.

TABLE 1. Comparison of wild-type and IGnT-deficient mice[a]

Parameter	Mean ± SD		Significance (*P*)
	WT mice	KO mice	
Spontaneous activity (10^2)			
Total activity			
Male ($n = 6^a$)	192.0 ± 9.9	93.6 ± 9.8	<0.05
Female ($n = 6$)	239.4 ± 12.3	166.1 ± 7.5	<0.05
Daytime activity (male, $n = 6$)	116.5 ± 8.9	69.8 ± 7.3	<0.05
Nighttime activity (male, $n = 6$)	99.2 ± 9.8	60.0 ± 9.0	<0.05
Blood cell count (10^6/ml)			
Red blood cells, 2 mo ($n = 12$)	$(1.10 \pm 0.1) \times 10^4$	$(1.17 \pm 0.2) \times 10^4$	NS
White blood cells			
2 mo ($n = 12$)	6.52 ± 0.25	2.47 ± 0.311	<0.01
6 mo ($n = 12$)	6.88 ± 0.57	4.68 ± 0.42	<0.01
Lymphocytes, 6 mo ($n = 12$)	5.76 ± 0.43	3.56 ± 0.25	<0.01
Neutrophils, 6 mo ($n = 12$)	1.11 ± 0.12	1.12 ± 0.11	NS
Monocytes, 6 mo ($n = 12$)	0.10 ± 0.01	0.10 ± 0.01	NS
Serum analysis (mg/ml)			
BUN			
2 mo ($n = 10$)	0.21 ± 0.04	0.29 ± 0.05	<0.05
6 mo ($n = 10$)	0.24 ± 0.05	0.33 ± 0.07	<0.01
Creatinine			
2 mo ($n = 10$)	31.2 ± 3.6	75.4 ± 7.7	<0.05
6 mo ($n = 10$)	81.5 ± 8.5	136.6 ± 14.1	<0.01
Glucose			
2 mo ($n = 21$)	1.28 ± 0.50	0.95 ± 0.55	NS
6 mo ($n = 21$)	1.31 ± 0.48	1.21 ± 0.53	NS

[a] *n*, number of mice analyzed for a genotype. NS, not significant; WT, wild type; KO, knockout.

4F). RT-PCR analysis of IGnT transcript revealed strong expression in B cells from the spleen, medium level of expression in T cells, and weak expression in granulocytes from blood (Fig. 4G). The difference between I antigen expression and IGnT expression in granulocytes is probably due to the difference in the source of the cells, namely, the spleen and blood. In any event, strong expression of I antigen in B cells is consistent with the phenotype in the deficient mice. We also examined possible differences in antibody production between wild-type and deficient mice. After 1,000 times dilution, anti-ovalbumin sera produced by wild-type mice gave an optical density of 0.202 ± 0.165, while that produced by the deficient mice gave OD an optical density of 0.142 ± 0.108. The difference was statistically not significant. The result indicates that in the deficient mice, B cells functioned normally, even though their number decreased. Probably, more mice are needed to yield statistically significant difference.

Decreased renal function in IGnT-deficient mice. We found that levels of both BUN and serum creatinine were significantly increased in deficient mice compared to wild-type mice (Table 1). The increase was observed both in 2-month-old and in 6-month-old mice. However, no significant difference was detected in the blood serum glucose concentration between the deficient and wild-type mice (Table 1). We also found vacuolization in tubular epithelial cells of 8-month-old deficient mice (Fig. 5). No obvious vacuolization was observed in the cells of 2-month-old mice, and a low level was detected in the cells of 4-month-old deficient mice.

Decreased lysosomal membrane proteins in the kidney of the deficient mice. In order to investigate the molecular mechanisms of the vacuolization and decreased renal function in IGnT-deficient mice, we analyzed the levels of lysosomal membrane proteins, LAMP-2, and synaptotagmins II and VII (2, 5, 30, 32). LAMP-1 and -2, closely related molecules, are major carriers of poly-*N*-acetyllactosamines (5), and mice deficient in LAMP-2 accumulate autophagic vacuoles (32). On the other hand, synaptotagmin VII has been identified as a key molecule in the repair of damaged cell membranes by lysosomes (30). Western blot analysis revealed the levels of LAMP-1 and -2 in the kidney to be significantly decreased in the deficient mice compared to wild-type mice (Fig. 6A). Furthermore, we noticed that the electrophoretic mobilities of LAMP-1 and -2 from the deficient mice were altered and became much sharper; the observation suggested that carbohydrates in LAMP-1 and -2 were altered in these animals. To confirm that the carbohydrates were actually altered, we isolated LAMP-2 by indirect immunoprecipitation and subjected it to SDS-PAGE with a 6% running gel. Under these conditions, the difference between LAMP-2 from wild-type and that from the deficient mice became clearer (Fig. 6B). Furthermore, the band from wild-type mice was stained by anti-I antibody, but the band from the deficient mice was scarcely stained.

The levels of synaptotagmins II and VII were also significantly decreased compared to those in wild-type mice (Fig. 7). The decrease of LAMP-2 appears to be related to vacuolization, whereas that of synaptotagmin VII is expected to be the principal reason for the renal dysfunction in the deficient mice. These points will be dealt with fully in the Discussion. In addition, it should be noted that a deficiency of poly-*N*-acetyllactosamine branching resulted in decreases in all four lysosomal membrane proteins examined.

Epidermoid cyst formation in IGnT-deficient mice. Male $IGnT^{-/-}$ mice frequently developed epidermoid cysts in the abdominal skin (Fig. 8A and B). This was first observed in

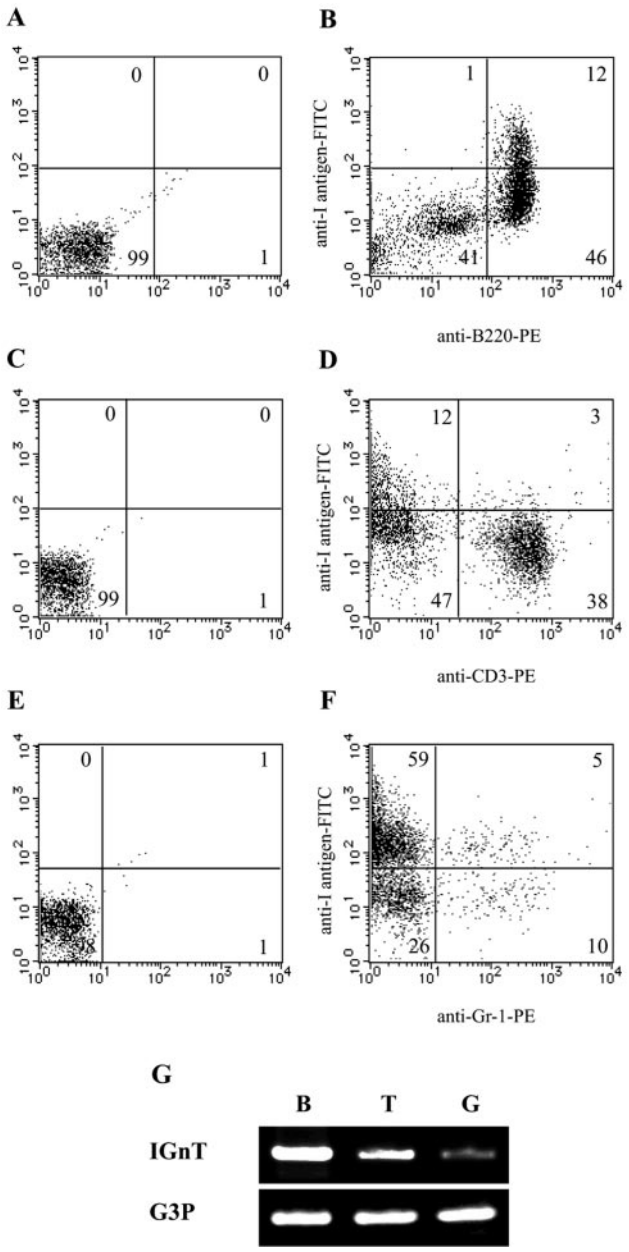

FIG. 4. Expression of I antigen and IGnT in murine leukocytes. (A to F) Analysis of spleen cells by flow cytometry. Cells were doubly stained with anti-B220-PE (B), anti-CD3-PE (D), or anti-Gr-1-PE (F) and OSK-14 anti-I antibody, followed by FITC-labeled anti-human IgM. Panels A, C, and E show unstained cells corresponding to panels B, D, and F, respectively. (G) RT-PCR analysis of IGnT and G3P expression in B and T cells from the spleen and blood granulocytes.

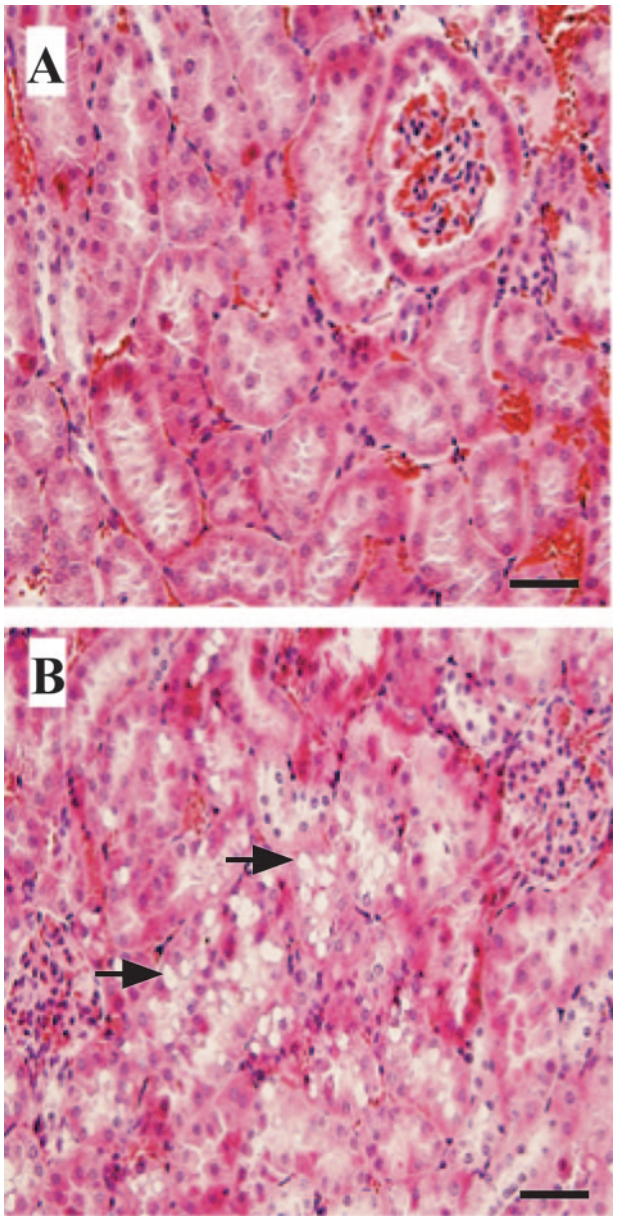

FIG. 5. Histological analysis of the kidney of 8-month-old male mice. Tissue sections were stained with HE. (A) Wild-type mice; (B) IGnT-deficient mice. Arrows show vacuolization. Bar, 50 μm.

3-month-old deficient mice. Until 8 months after birth, the incidence of epidermoid cysts increased to ca. 50%. The incidence did not increase further, when the observation period was extended till 12 months after birth. The size of the cysts increased during the period. Epidermoid cysts were not observed in wild-type mice or female IGnT-deficient mice.

Cataracts did not develop earlier in IGnT-deficient mice. Figure 8C shows representative slit-lamp images of the lens at different ages and after consumption of the diet containing 50% galactose. Eight-week-old mice (8-W) exhibited no cataractous changes (score 0). Forty-week-old mice (40-W) showed mild cataracts in the cortical regions (score 1). However, there was no difference in the degree of lens opacity between wild-type and deficient mice. Although observations were continued till 55 weeks after birth, cataracts did not become more severe in mice of either genotype. In order to induce cataracts, the 4-week-old mice were also fed a 50% galactose-containing diet for 8 weeks (12-W+Gal), but significant lens opacity was not seen for wild-type or deficient mice (score 0).

DISCUSSION

Three spliced forms of IGnT are present in humans and mice, and all share common exons (4, 6, 11, 34, 40, 41). We

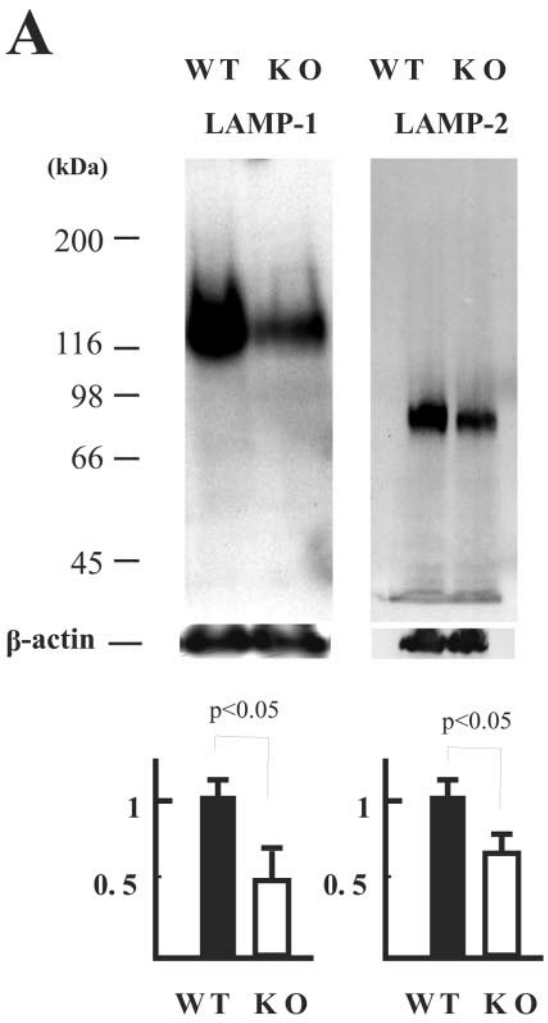

FIG. 6. Alteration of LAMP-1 and -2 expression by IGnT deficiency. (A) Estimation of LAMP-1 and -2 levels in the kidneys of 6-month-old male mice by Western blot analysis. The intensity of bands determined by densitometry was normalized to that of β-actin. The results are shown as a ratio to the value for wild-type mice (n = 4, WT, closed bar). The value in the deficient mice (n = 4, KO) is shown by an open bar. (B) Alteration of carbohydrate portion of LAMP-2. LAMP-2 isolated from the kidney of wild-type or deficient mice by immunoprecipitation was subjected to SDS-PAGE by using 6% gel and blotted with anti-LAMP-2 or anti-I antibody.

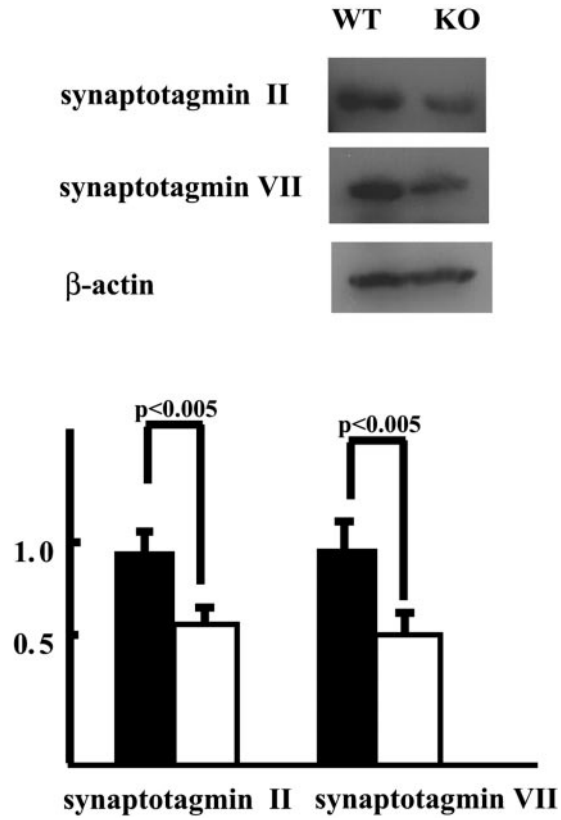

FIG. 7. Estimation of synaptotagmin II and VII levels in the kidney of 6-month-old male mice by Western blot analysis. The intensity of bands determined by densitometry was normalized to that of β-actin. The results are shown as a ratio to the value for wild-type mice (n = 4, WT, solid bar). The value in the deficient mice (n = 4, KO) was shown by an open bar.

have deleted the major common exon of IGnTs in the present study. Indeed, IGnT activity was abolished in the stomachs, kidneys, bone marrow, and cerebella of deficient mice. A small amount of IGnT activity detected in the small intestine of the deficient mice was considered to be due to Core2GlcNAcT-II (38). These results confirmed that the three spliced forms of IGnT are the principal poly-*N*-acetyllactosamine-branching enzymes in adult mice.

Immunohistochemical staining with an anti-I monoclonal antibody OSK-14 revealed that I antigenic activity disappeared from the kidneys and stomachs of deficient mice. A weak antigenic activity remained in the small intestine of the deficient mice. These results are consistent with the activity levels of IGnT determined in vitro. However, I antigen was not detected in the cerebellum of wild-type mice, even though IGnT activity was detected in the homogenate of the cerebel-

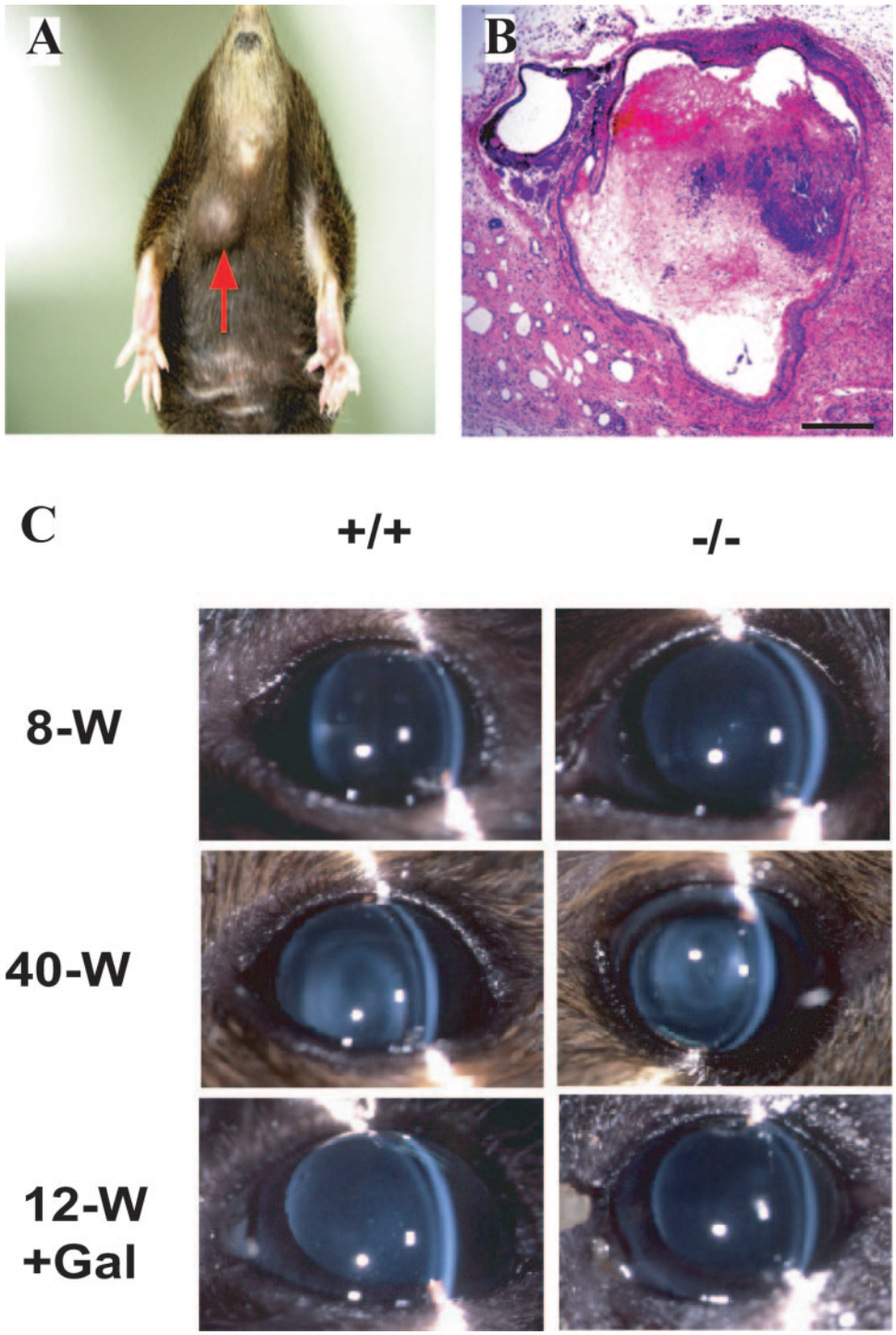

FIG. 8. Spontaneous epidermoid cyst in an IGnT-deficient mouse and examination of possible occurrence of cataracts in IGnT-deficient mice. (A) External view of the tumor in an 8-month-old male IGnT-deficient mice. (B) A section of the tumor stained with HE. Bar, 50 μm. (C) Slit-lamp images of the lenses in wild-type (left) and the deficient (right) mice. 8-W, 8-week-old mice. For a genotype, six mice were examined and gave the same result (score 0). 40-W, 40-week-old mice. For a genotype, four mice were examined and gave the same result (score 1). 12-W+Gal, 12-week-old mice after being fed a 50% galactose-containing diet. For a genotype, two mice were examined and gave the same result (score 0).

lum and IGnT mRNA was detected in the organ by RT-PCR. Further investigation revealed that 4C9 antigen, a Lewis X antigen, was expressed strongly in the glomeruli of the granular layer of the cerebellum but only very weakly in that of deficient mice. Most probably, OSK-14 antibody cannot recognize I structure, when its nonreducing ends are covered by Lewis X structure. Furthermore, the result suggests that a high density of the Lewis X epitope accomplished by branching of the

backbone structure is required for strong expression of 4C9 antigen. In this context, it should be mentioned that the mode of expression of 4C9 antigen is more restricted than that of the typical Lewis X antigen, SSEA-1, during mouse embryogenesis (39). In the mouse brain, SSEA-1 is expressed in several areas, including the cerebrum (26), whereas we noted that 4C9 antigen was expressed only in the site described above.

A high-molecular-weight branched poly-*N*-acetyllactosamine called embryoglycan is abundantly expressed during early embryonic stages in mice and carries a number of carbohydrate epitopes such as Lewis X (14, 24, 29). However, the IGnT-deficient mice studied here were born with the expected Mendelian ratio and reproduced well when the homozygous deficient mice were mated with each other. IGnT transcripts are strongly expressed in embryonal carcinoma cells and ES cells, which resemble multipotential cells of early embryos (4, 6). Therefore, there is little doubt that IGnT knocked out in the present investigation plays significant roles in the production of embryoglycan. An unresolved issue is whether some other enzyme(s) compensates for the loss of IGnT in early embryonic cells. Core2GlcNAcT-II is a candidate for such an enzyme. Thus, further studies are required to decide whether embryoglycan plays critical roles in embryogenesis. In this context, it should be also pointed out that Lewis X epitope on embryoglycan appears to be unnecessary during the early embryonic period, since knockout of fucosyltransferase IX, which is responsible for the formation of Lewis X during this period, does not impair embryogenesis (17).

The IGnT-deficient mice exhibited reduced spontaneous movement. However, their physical capability estimated by using the rota-rod test was normal. Although a deficit in high-order mental activity such as the desire to move or explore is not excluded, it is possible that the decreased activity is a consequence of systemic weakness. Indeed, the deficient mice showed lowered B lymphocyte numbers in the blood and elevated BUN and creatinine levels. Renal tubular epithelial cells tended to form vacuoles in the aging deficient mice. We also noted epidermoid cysts in male deficient mice after half a year of life. No epidermoid cysts were found in female deficient mice. It is worth noting that in collagenase-2-deficient mice, epidermoid cysts also only occurred in the males and effects of sex hormones are considered to explain the phenomenon (1).

Clues to the molecular basis of the abnormalities were obtained regarding vacuolization and reduced kidney function. We found that the levels of 4 lysosomal proteins, LAMP-1 and -2 and synaptotagmins II and VII, were significantly reduced in the kidney of IGnT-deficient mice compared to those in the kidney of wild-type mice. Two closely related molecules, LAMP-1 and -2, are important carriers of poly-*N*-acetyllactosamines and are located in the lysosomal membrane (5). A lack of poly-*N*-acetyllactosamine branching may reduce the stability of LAMP-2, leading to a decrease in the amount of the molecule. In relation to this hypothesis, the importance of N glycosylation to the stability of LAMP-1 has been demonstrated: LAMP-1 synthesized in the presence of tunicamycin has a decreased half-life (3). That carbohydrates of LAMP-2 were actually altered in the kidney of the deficient mice was evident from the altered electrophoretic mobility and the loss of I antigen. The decrease of LAMP-2 can be correlated with vacuolization, since it has recently been shown that autophagic vacuoles accumulate extensively in LAMP-2-deficient mice (32). Although vacuolization occurs in many organs in LAMP-2-deficient mice (32), it was confined to the kidney in IGnT-deficient mice. The decrease but not loss of LAMP-2 in IGnT-deficient mice probably affected only the most susceptible organ.

A damaged plasma membrane is sealed by the lysosomal membrane, and synaptotagmin VII plays important roles in the process (30): anti-synaptotagmin VII or a fragment of synaptotagmin VII inhibits the sealing. Thus, a decrease in synaptotagmin VII can affect the repair of renal epithelial cells, leading to renal dysfunction. The carbohydrate portion of synaptotagmin VII is not yet known. However, the fact that levels of all four lysosomal membrane proteins decreased indicates a common mechanism behind the decrease. Most probably, branched poly-*N*-acetyllactosamines are present also on synaptotagmin II and VII and increase their stability. Alternatively, LAMPs associate with synaptotagmins and increase their stability. In any event, we believe that the decrease of lysosomal membrane proteins in the absence of branched poly-*N*-acetyllactosamine is the key event causing abnormalities in the kidney of the deficient mice.

In Asian populations, i blood group phenotype of erythrocytes is clearly associated with the onset of cataracts, while the relationship is less clear in Caucasian populations (18, 19, 22, 28, 37). IGnT C (IGnT3) is responsible for I antigen expression on erythrocytes (11, 41). Null mutation of IGnT C can occur either in exon I, which is specific for IGnT C, or in exon II or III, which are shared by other IGnTs. In the former case, I antigen will disappear only from restricted cells including erythrocytes. In the latter case, I antigen will disappear from many types of cells. A recent genetic analysis found that all of five individuals with i blood group and with congenital cataracts had null mutations in the common exon, whereas an individual with i blood group and without congenital cataracts had a mutation in the exon specific for IGnT C (41). The results suggest that a lack of all spliced variants of IGnTs causes cataracts in humans. However, the IGnT-deficient mice studied here did not exhibit an increased susceptibility to cataracts even in aged animals, in which slight turbidity was observed in the lenses of both wild-type and deficient mice. Thus far, age-related phenotypes of the deficient mice have been observed in terms of cyst development and vacuolization of renal tubular epithelial cells; the incidence increased till 8 months after birth. Apparently, an age-related occurrence of the phenotype did not happen upon the formation of cataracts.

It should be noted that the lens epithelial cells of mice express the IGnT B transcript (34), one of the three IGnTs deleted in the present study. Thus, we should take into account the possibility that the loss of IGnT is not the reason for the development of cataracts in humans, and the mutation of a closely linked gene is responsible (41). A more likely explanation is that a difference in the expression of other glycosyltransferases in lens epithelial cells is responsible for the difference of the phenotype between humans and mice.

Likewise, to the best of our knowledge, we do not know of abnormalities other than cataracts in individuals with i blood group. Although it is quite possible that abnormalities were overlooked in the rare individuals who lacked all spliced variants of IGnTs, it is likely that stronger expression of some

glycosyltransferases in certain tissues of humans concealed the expression of phenotypes. An obvious candidate for such an enzyme is Core2GlcNAcT-II. Our current hypothesis is that branched poly-*N*-acetyllactosamines increase the amount of some lysosomal proteins and contribute to an increase of cell survival and that a species difference in the mode of expression of other glycosyltransferases affects the tissue in which abnormalities are found upon IGnT deficiency.

ACKNOWLEDGMENTS

We are much indebted to R. Kannagi and L. Chen for cooperation in analysis of I antigen and IGnT mRNA in leukocytes. We also thank T. Yamano for the generous gift of OSK-14 antibody and T. Adachi and H. Inoue for secretarial assistance.

This study was supported by a grant from the Ministry of Education, Culture, Sports, Science, and Technology of Japan (grant 14082202).

REFERENCES

1. **Balbín, M., A. Fueyo, A. M. Tester, A. M. Pendás, A. S. Pitiot, A. Astudillo, C. M. Overall, S. D. Shapiro, and C. López-Otín.** 2003. Loss of collagenase-2 confers increased skin tumor susceptibility to male mice. Nat. Genet. **35:** 252–257.
2. **Baram, D., R. Adachi, O. Medalia, B. F. Dickey, Y. A. Mekori, and R. Sagi-Eisenberg.** 1999. Synaptotagmin II negatively regulates Ca^{2+}-triggered exocytosis of lysosomes in mast cells. J. Exp. Med. **189:**1649–1658.
3. **Barriocanal, J. G., J. S. Bonifacino, L. Yuan, and I. V. Sandoval.** 1986. Biosynthesis, glycosylation, movement through the Golgi system, and transport to lysosomes by an N-linked carbohydrate-independent mechanism of three lysosomal integral membrane proteins. J. Biol. Chem. **261:**16755–16756.
4. **Bierhuizen, M. F. A., M.-G. Mattei, and M. Fukuda.** 1993. Expression of the developmental I antigen by a cloned human cDNA encoding a member of a β-1,6-*N*-acetylglucosaminyltransferase gene family. Genes Dev. **7:**468–478.
5. **Carlsson, S. R., J. Roth, F. Piller, and M. Fukuda.** 1988. Isolation and characterization of human lysosomal membrane glycoproteins, h-lamp-1 and h-lamp-2: major sialoglycoproteins carrying polylactosaminoglycan. J. Biol. Chem. **263:**18911–18919.
6. **Chen, G. Y., N. Kurosawa, and T. Muramatsu.** 2000. A novel variant form of murine β-1,6-*N*-acetylglucosaminyltransferase forming branches in poly-*N*-acetyllactosamines. Glycobiology **10:**1001–1011.
7. **Chylack, L. T., Jr., M. C. Leske, R. Sperduto, P. Khuand, and D. McCarthy.** 1988. Lens opacities classification system. Arch. Ophthalmol. **106:**330–334.
8. **Fukuda, M., M. N. Fukuda, and S. Hakomori. Developmental change and genetic defect in the carbohydrate structure of band 3 glycoprotein of human erythrocyte membrane.** 1979. J. Biol. Chem. **254**:3700–3703.
9. **Fukuda, M.** 1985. Cell surface glycoconjugates as onco-differentiation markers in hematopoietic cells. Biochim. Biophys. Acta **780:**119–150.
10. **Igakura, T., K. Kadomatsu, T. Kaname, H. Muramatsu, Q. W. Fan, T. Miyauchi, Y. Toyama, N. Kuno, S. Yuasa, M. Takahashi, T. Senda, O. Taguchi, K. Yamamura, K. Arimura, and T. Muramatsu.** 1998. A null mutation in basigin, an immunoglobulin superfamily member, indicates its important roles in peri-implantation development and spermatogenesis. Dev. Biol. **194:**152–165.
11. **Inaba, N., T. Hiruma, A. Togayachi, H. Iwasaki, X. H. Wang, Y. Furukawa, R. Sumi, T. Kudo, K. Fujimura, T. Iwai, M. Gotoh, M. Nakamura, and H. Narimatsu.** 2003. A novel I-branching β-1,6-*N*-acetylglucosaminyltransferase involved in human blood group I antigen expression. Blood **101:**2870–2876.
12. **Jarnefelt, J., J. Rush, Y. T. Li, and R. A. Laine.** 1978. Erythroglycan, a high molecular weight glycopeptide with the repeating structure [galactosyl-(1–4)-2-deoxy-2-acetamido-glucosyl(1–3)] comprising more than one-third of the protein-bound carbohydrate of human erythrocyte stroma. J. Biol. Chem. **253:**8006–8009.
13. **Kador, P. F., Y. Akagi, and J. H. Kinoshita.** 1986. The effect of aldose reductase and its inhibition on sugar cataract formation. Metabolism **35:**15–19.
14. **Kamada, Y., Y. Arita, S. Ogata, H. Muramatsu, and T. Muramatsu.** 1987. Receptors for fucose-binding proteins of *Lotus tetragonolobus* isolated from mouse embryonal carcinoma cells. Structural characteristics of the poly(*N*-acetyllactosamine)-type glycan. Eur. J. Biochem. **163:**497–502.
15. **Kapadia, A., T. Feizi, and M. J. Evans.** 1981. Changes in the expression and polarization of blood group I and i antigens in post-implantation embryos and teratocarcinomas of mouse associated with cell differentiation. Exp. Cell Res. **131:**185–195.
16. **Krusius, T. J. Finne, and H. Rauvala.** 1978. The poly(glycosyl) chains of glycoproteins: characterisation of a novel type of glycoprotein saccharides from human erythrocyte membrane. Eur. J. Biochem. **92:**289–300.
17. **Kudo, T., M. Kaneko, H. Iwasaki, A. Togayachi, S. Nishihara, K. Abe, and H. Narimatsu.** 2004. Normal embryonic and germ cell development in mice lacking α 1,3-fucosyltransferase IX (Fut9) which show disappearance of stage-specific embryonic antigen 1. Mol. Cell. Biol. **24**:4221–4228.
18. **Lin-Chu, M., R. E. Broadberry, Y. Okubo, and M. Tanaka.** 1991. The i phenotype and congenital cataracts among Chinese in Taiwan. Transfusion **31:**676–677.
19. **Macdonald, E. B., R. Douglas, and P. A. Harden.** 1983. Caucasian family with the i phenotype and congenital cataracts. Vox Sang **44:**322–325.
20. **Magnet, A. D., and M. Fukuda.** 1997. Expression of the large I antigen forming β-1,6-*N*-acetylglucosaminyltransferase in various tissues of adult mice. Glycobiology **7:**285–295.
21. **Marsh, W. L., and W. J. Jenkins.** 1960. Anti-i: a new cold antibody. Nature **188:**753.
22. **Marsh, W. L., and H. DePalma.** 1982. Association between the Ii blood group and congenital cataract. Transfusion **22:**337–338.
23. **Muramatsu, T.** 1988. Developmentally regulated expression of cell surface carbohydrates during mouse embryogenesis. J. Cell. Biochem. **36:**1–14.
24. **Muramatsu, T., G. Gachelin, M. Damonneville, C. Delarbre, and F. Jacob.** 1979. Cell surface carbohydrates of embryonal carcinoma cells: polysaccharidic side chains of F9 antigens and of receptors to two lectins, FBP and PNA. Cell **18:**183–191.
25. **Muramatsu, T., G. Gachelin, J. F. Nicolas, H. Condamine, H. Jakob, and F. Jacob.** 1978. Carbohydrate structure and cell differentiation: unique properties of fucosyl-glycopeptides isolated from embryonal carcinoma cells. Proc. Natl. Acad. Sci. USA **75:**2315–2319.
26. **Nishihhara, S., H. Iwasaki, K. Nakajima, A. Togayachi, Y. Ikehara, T. Kudo, Y. Kushi, A. Furuya, K. Shitara, and H. Narimatsu.** 2003. α-1,3-Fucosyltransferase IX (Fut9) determines Lewis X expression in brain. Glycobiology **13:**445–455.
27. **Nomoto, S., H. Muramatsu, M. Ozawa, T. Suganuma, M. Tashiro, and T. Muramatsu.** 1986. An anti-carbohydrate monoclonal antibody inhibits cell-substratum adhesion of F9 embryonal carcinoma cells. Exp. Cell Res. **164:** 49–62.
28. **Ogata, H., Y. Okubo, and T. Akabane.** 1979. Phenotype i associated with congenital cataract in Japanese. Transfusion **19:**166–168.
29. **Ozawa, M., T. Muramatsu, and D. Solter.** 1985. SSEA-1, a stage-specific embryonic antigen of the mouse, is carried by the glycoprotein-bound large carbohydrate in embryonal carcinoma cells. Cell Differ. **16:**169–173.
30. **Reddy, A., V. Caler, and N. W. Andrews.** 2001. Plasma membrane repair is mediated by Ca^{2+}-regulated exocytosis of lysosomes. Cell **106:**157–169.
31. **Sakamoto, Y., T. Taguchi, Y. Tano, T. Ogawa, A. Leppanen, M. Kinnunen, O. Aitio, P. Parmanne, O. Renkonen, and N. Taniguchi.** 1998. Purification and characterization of UDP-GlcNAc:Galβ1-4GlcNAcbeta1-3*Galβ1-4Glc-(NAc)-R(GlcNAc to *Gal) β1,6N-acetylglucosaminyltransferase from hog small intestine J. Biol. Chem. **273:**27625–27632.
32. **Tanaka, Y., G. Guhde, A. Suter, E. L. Eskelinen, D. Hartmann, R. L. Rauch, P. M. Janssen, J. Blanz, K. Figura, and P. Saftig.** 2000. Accumulation of autophagic vacuoles and cardiomyopathy in LAMP-2-deficient mice. Nature **406:**902–906.
33. **Turunen, J. P., M.-L. Majuri, A. Seppo, S. Tiisala, T. Paavonen, M. Miyasaka, K. Lemström, L. Penttilä, O. Renkonen, and R. Renkonen.** 1995. De novo expression of endothelial sialyl Lewis (a) and sialyl Lewis (x) during cardiac transplant rejection: superior capacity of a tetravalent sialyl Lewis (x) oligosaccharide in inhibiting L-selectin-dependent lymphocyte adhesion. J. Exp. Med. **182**:1133–1142.
34. **Twu, Y. C., M.-L Chou, and L.-C. Yu.** 2003. The molecular genetics of the mouse I β-1,6-*N*-acetylglucosaminyltransferase locus. Biochem. Biophys. Res. Commun. **303:**868–876.
35. **Varki, A., R. Cummings, J. Esko, H. Freeze, G. Hart, and J. Marth (ed.)** 1999. Essentials of glycobiology. Cold Spring Harbor Laboratory Press, Cold Spring Harbor, N.Y.
36. **Watanabe, K., S. I. Hakomori, R. A. Childs, and T. Feizi.** 1979. Characterization of a blood group I-active ganglioside: structural requirements for I and i specificities. J. Biol. Chem. **254:**3221–3228.
37. **Yanaguchi, H., Y. Okubo, and M. Tanaka.** 1972. A note on possible close linkage between the Ii blood locus and a congenital cataract locus Proc. Jpn. Acad. **48:**625–628.
38. **Yeh, J.-C., E. Ong, and M. Fukuda.** 1999. Molecular cloning and expression of a novel β-1,6-*N*-acetylglucosaminyltransferase that forms core 2, core 4, and I branches. J. Biol. Chem. **274:**3215–3221.
39. **Yoshinaga, K., H. Muramatsu, and T. Muramatsu.** 1991. Immunohistochemical localization of the carbohydrate antigen 4C9 in the mouse embryo: a reliable marker of mouse primordial germ cells. Differentiation **48:**75–82.
40. **Yu, L.-C., Y.-C. Twu, C.-Y. Chang, and M. Lin.** 2001. Molecular basis of the adult i phenotype and the gene responsible for the expression of the human blood group I antigen. Blood **98:**3840–3845.
41. **Yu, L.-C. Y.-C. Twu, M.-L. Chou, M. E. Reid, A. R. Gray, J. M. Moulds, C.-Y. Chang, and M. Lin.** 2003. The molecular genetics of the human I locus and molecular background explain the partial association of the adult i phenotype with congenital cataracts. Blood **101:**2081–2088.